An experimental study on a compliant floating platform with a front barrier under wave action

Bi, Cheng; Law, Adrian Wing-Keung

2022

Bi, C. & Law, A. W. (2022). An experimental study on a compliant floating platform with a front barrier under wave action. 37th International Conference on Coastal Engineering (ICCE 2022).

https://hdl.handle.net/10356/161625

An Experimental Study on a Compliant Floating Platform with a Front Barrier under Wave Action

Cheng Bi, Nanyang Technological University, cheng018@e.ntu.edu.sg
Adrian Wing-Keung Law, Nanyang Technological University, cwklaw@ntu.edu.sg

INTRODUCTION

In recent years, solar power production has become the major source of renewable energy to combat climate change (Sahu et al., 2016), and floating solar farms (FSFs) are being explored on water space such as reservoirs and lakes at various major cities (Bi et al., 2021). Compared to the traditional ground-based solar farm, FSF requires no land use and the power generation efficiency can be increased potentially due to the water-cooling effect (Golroodbari and van Sark, 2020). In addition, the coastal environment with more water space is also being considered for future development of FSF. With coastal floating solar farms, the PV panels can be supported on top of a compliant platform consisting of interconnected floating modules (Dai et al. 2020). However, excessive displacement of the platform can be induced by the incident wave action which can affect its structural stability (Sree et al., 2022). In this study, we examine the use of a submerged tensioned barrier installed in front of the FSF at a finite distance to stabilize the floating platform. Experiments were conducted to investigate the effectiveness of this protection measure. The effects of barrier length, platform length, and spacing between the barrier and platform on the displacement of the platform are investigated with respect to the wave transmission and reflection. In the following, we shall briefly describe the experimental setup and show some of the results obtained.

EXPERIMENTAL SETUP

The experiments were conducted in a wave flume which was 35m long, 0.55m wide and 0.6m deep as shown in Figure 1 at the Hydraulics Laboratory, School of Civil and Environmental Engineering, Nanyang Technological University. The flume was equipped with a flap-type monochromatic wavemaker, and mesh-type wave absorbers were installed at the flume end with a slope of 1:13 on top of a beach.

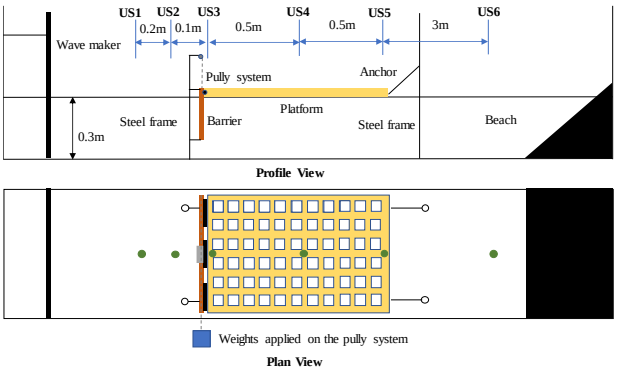

Figure 1. Schematic diagram of experimental setup

A 1:30 scale was used to model the conversion from the field to laboratory conditions. The prototype module dimensions and material characteristics were obtained from the patent PCT/SG2019/050220 for the FSF developed by the Housing & Development Board (HDB), Singapore. The prototype module was hollow with a shell thickness of 3mm and it was impossible to emulate the shell structure in the laboratory scale. Thus, a solid module made of a 7mm thick ethylene-vinyl acetate (EVA) foam sheet with the same dimensions and equivalent bending stiffness was used instead, and the corresponding scaled-down elastic modulus was determined as ~ 4 MPa. The sheet was also perforated to simulate the global array of the FSF consisting of interconnected floating modules. Two sheet lengths, 1m and 2m, were considered corresponding to 15 modules and 31 modules along the longitudinal direction, respectively, with the same width of 0.53m corresponding to 7 modules in the lateral direction. The vertical barrier was made of a 2mm thick polypropylene board with the elastic modulus of 1100 MPa. The barrier was hinged and held by a steel frame with a pully system to apply the tension though a weight. The weight was constant at 10 kg for all the cases corresponding to the nondimensional tensions per unit width $Q/\rho g h^2$ of 0.2, where ρ is the water density, g the gravitational acceleration and h the water depth. The barrier material and the tension magnitude were selected so that the barrier fell within the regime of flexible membrane as defined by Bi et al. (2022) where the bending stiffness and tension effect are comparable in the dynamic response of the barrier. When the spacing between the barrier and platform was finite, the platform was anchored with the spring at four corners. When there was no spacing, the platform was directly connected to the barrier through hinges at the leading edge and anchored at the other end with two springs of 2.5 kN/mm stiffness.

Ultrasound sensors (US325, General Acoustics) with a resolution of 0.18 mm and sampling frequency of 50 Hz were installed on top and around the floating platform to monitor the surface displacement under the wave action. They were synchronized by a common data acquisition system (NI 9215, National Instruments), and the time series data were recorded using LABVIEW. Two ultrasound sensors were installed in front of the barrier to quantify the incident and reflected waves while three sensors were placed on top of the platform to measure the platform displacement at the two ends as well as the middle point. Finally, one sensor was placed behind the platform to measure the wave transmission.

The water depth and incident wave amplitude were kept constant at 0.3m and 0.011m, respectively, and periods of the incident wave ranged from 0.5s to 1s with the increment of 0.05s. The corresponding prototype

conditions are typical for the coastal environment with such FSF installations based on our experience.

RESULTS

Figure 2 shows the reflection (R_r) and transmission (T_r) coefficient against the incident wave period for different barrier penetration ratio, d/h, where d is the barrier length and h is the water depth. In this case, the perforated platform had a length of L/h=3.3 and the spacing between the platform and barrier is zero. It can be seen that the overall R_r decreases while T_r increases as the incident wave period increases due to more wave transmission through the gap below the barrier for longer waves. Moreover, T_r reduces as the barrier length increases. In particular, a significant reduction in T_r occurs when d/h increases from 0.2 to 0.4, and the reduction becomes less obvious when d/h further increases to 0.6, especially for smaller wave periods (e.g. 0.55 – 0.8s). This indicates that the use of a barrier with a length of 40% - 60% of the water depth can reflect a significant amount of incident waves and thus reduce the wave energy transmitted to the floating platform under the test conditions.

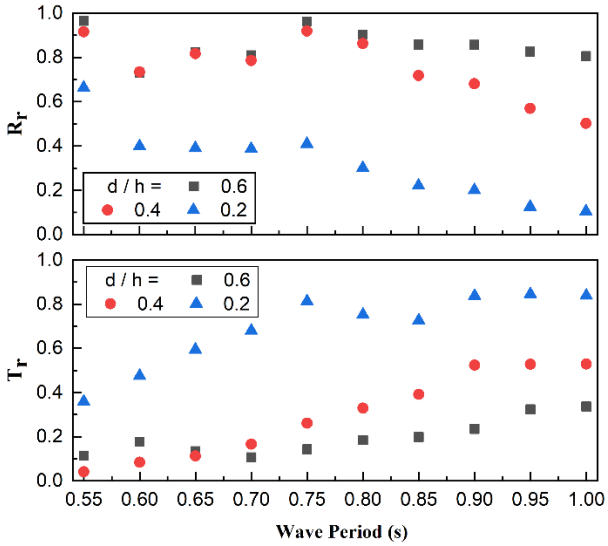

Figure 2. Reflection and transmission coefficient against wave period for different barrier penetration ratios

Figure 3 plots R_r and T_r against the incident wave period for different nondimensional barrier-platform spacings L_d/h. In this case, the perforated platform had a length of L/h = 3.3 and the barrier had a length of d/h = 0.6. It is observed that the increase of L_d/h from 0 to 3.3 results in only small changes of both wave reflection and transmission. Since the barrier with the penetration ratio of 0.6 is relatively long and rigid, most of the wave energy is reflected and thus the spacing does not have much effect on wave transmission despite more trapped waves between the barrier and platform.

Figure 4 shows R_r and T_r against the incident wave period for different nondimensional platform length L/h. In this case, the barrier has a length of d/h = 0.6 and the barrier-platform spacing is zero. It can be seen that the effect of platform length is negligible within the measured range of wave periods.

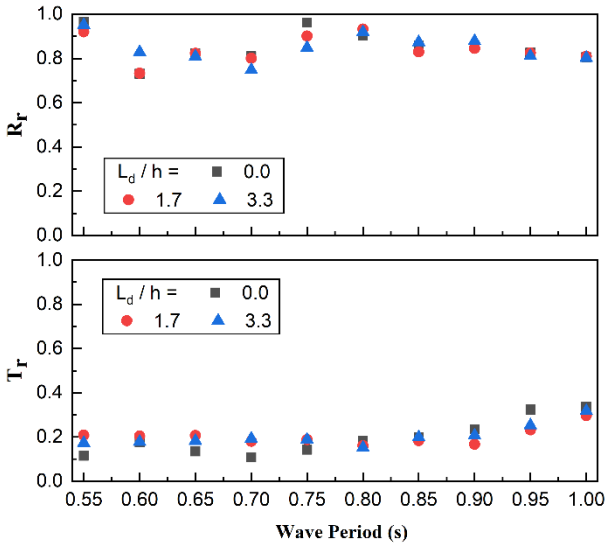

Figure 3. Reflection and transmission coefficient against wave period for different spacings

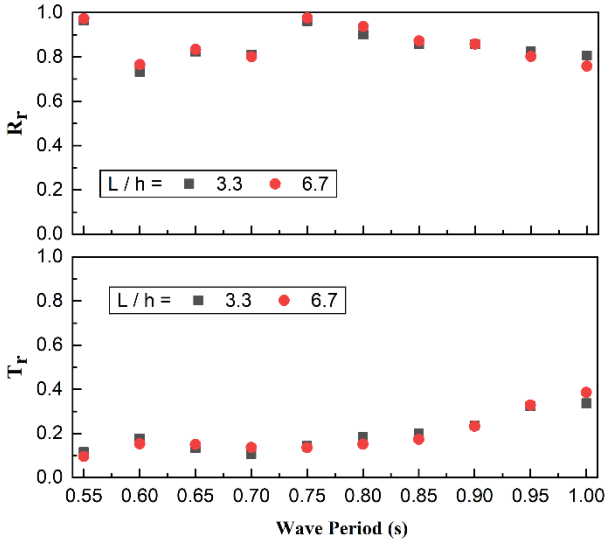

Figure 4. Reflection and transmission coefficient against wave period for different platform lengths

Figure 5 shows the displacement amplitude at the mid-point of the floating platform against wave period under the effects of three variables: barrier length, spacing and platform length. In all the subfigures, the black square represents the wave interaction with a single platform without the barrier (i.e. d/h=0 for Figure 5(a) as well as no barrier case for Figure 5(b) and (c)). Figure 5(a) plots the effect of barrier length on the platform motion. The results show that with the smaller wave periods from 0.55 to 0.70 s, a significant reduction of the platform displacement can be achieved by using a barrier even with a shallow penetration ratio of 0.2 compared to the

single platform case, and the reduction becomes larger as the barrier length increases. Moreover, the difference between the two cases of d/h = 0.4 and 0.6 is small for shorter waves, which is consistent with the trend of transmission coefficient. When the wave period further increases, however, a longer barrier of d/h = 0.4 or more is needed for stabilizing the floating platform due to the wave diffraction through the gap below the barrier, and the difference between the barrier penetration of 0.4 and 0.6 becomes more obvious.

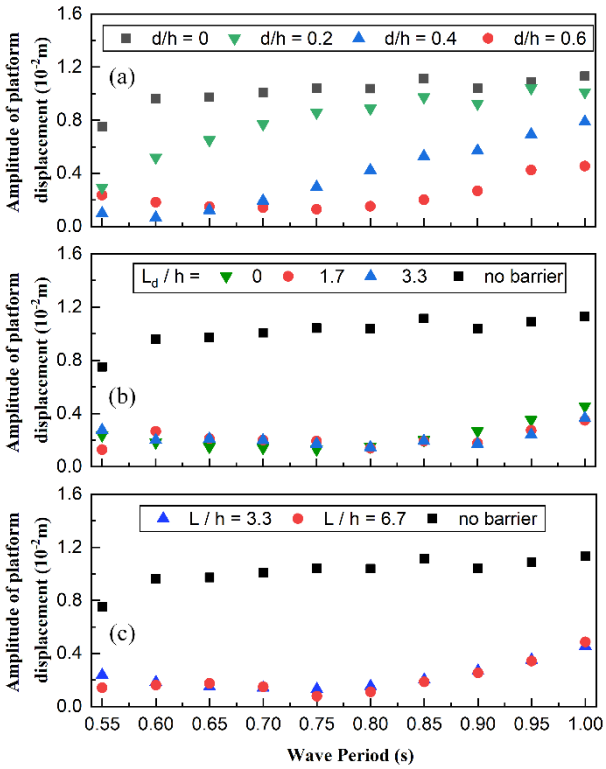

Figure 5. Displacement amplitude of the platform at mid-point against wave periods for different (a) barrier length, (b) spacing and (c) platform length

Figure 5(b) shows the effect of the spacing between the barrier and platform on the platform displacement. The barrier and platform length are same as those in Figure 3. Similar to the trend of reflection and transmission coefficient in Figure 3, the spacing does not affect the platform motion significantly. Thus, the barrier can be attached closely to the floating platform in the real installation so that the platform can provide buoyancy to the barrier.

Figure 5(c) shows the effect of the platform length on the platform displacement. The spacing and barrier length are same as those in Figure 4. Again, similar to the change of the reflection and transmission coefficient in Figure 4, the platform length has almost negligible effect on its displacement due to its compliant structural characteristics.

CONCLUSION

In this study, experiments on the wave interaction with a barrier-platform system were conducted to investigate the performance of a tensioned flexible barrier on the stabilization of a floating compliant platform for FSF. Design variables such as the barrier penetration, spacing and platform length were examined to quantify their effects on the wave reflection and transmission and the platform motion. The experimental results show that the use of a tensioned barrier in the regime of flexible membrane with a penetration ratio of 0.4 - 0.6 can reduce the wave transmission and stabilize the platform significantly, especially in the range of smaller wave periods. As the incident wave period increases, the protection of the platform becomes less significant due to the wave transmission through the gap below the barrier. Moreover, the spacing between the barrier and platform has little effect within the measured wave periods. Hence, the attachment of the barrier to the platform front is recommended so that the platform can provide buoyancy to the barrier. Finally, the result with nondimensional platform length of 3.3 and 6.6 were similar due to the compliant nature of the platform.

REFERENCES

Bi, Wu, Law (2021). Stabilisation of compliant floating platforms with sheet barriers under wave action. Ocean Engineering, vol. 240, pp. 109933.

Bi, Wu, Law (2022). Surface wave interaction with a vertical viscoelastic barrier. Applied Ocean Research, vol. 120, pp. 103073.

Dai, Zhang, Lim, Ang, Qian, Wong, Tan, Wang, (2020). Design and construction of floating modular photovoltaic system for water reservoirs. Energy vol. 191, pp. 116549.

Golroodbari, van Sark (2020). Simulation of performance differences between offshore and land - based photovoltaic systems. Progress in Photovoltaics: Research and Applications, vol. 28(9), pp. 873-886.

Sahu, Yadav, Sudhakar, (2016). Floating photovoltaic power plant: A review. Renew. Sustain. Energy Rev., vol. 66, pp. 815-824.

Sree, Law, Pang, Tan, Wang, Kew, Seow, Lim (2022). Fluid-structural analysis of modular floating solar farms under wave motion. Solar energy, vol. 233, pp.161-181.